JMEPEG
https://doi.org/10.1007/s11665-022-06713-8

1059-9495/$19.00

TECHNICAL ARTICLE

A Comparative Study on Impact Wear of Diamond-Like Carbon Films on H62 and GCr15 Steel

Shaomiao Shi, Xubing Wei, Xia Li, Qinglin Li, Shiyan Ding, Chenglong Fan, Guangan Zhang, and Zhibin Lu

Submitted: 16 June 2021 / Revised: 13 January 2022 / Accepted: 13 January 2022

The impact wear resistance and reliability of Diamond-like carbon (DLC), Hydrogenated diamond-like carbon (HDLC) and Hydrogenated diamond-like carbon with WC transition layer (WC HDLC) films and their GCr15 and H62 substrates were evaluated by reproducible impact wear characterization method. The test results show that three film-substrate systems on H62 have obviously failure and severe impact deformation. However, three film-substrate systems on GCr15 possessed better impact wear resistance, compared to three film-substrate systems on H62. The fatigue failure resistance of the film increases with the increase in the substrate hardness. In addition, the impact force will increase as the hardness of the film on the soft substrate increases, but the hardness of the film on the hard substrate has little effect on the impact force. Among six film-substrate systems tested, HDLC films with low hardness and high adhesion regardless of whether the substrate is soft or hard are most suitable for applications involving impact dynamic loads.

Keywords diamond-like carbon film, dynamic response, failure mechanisms, impact wear resistance

1. Introduction

Lubricating materials are of particular interest for saving energy and protecting environment, because friction and wear cause much energy loss, especially in the engineering field (Ref 1-4). Diamond-like carbon (DLC) have become a promising solid lubricant material because of its high strength, wear-resistance, high hardness, friction-reduction and corrosion resistance (Ref 5-10). Hence, it was widely used in cutting tools, automotive engines, biomedicines and other fields (Ref 4, 11-20). Besides, by doping metal atoms and/or mixing hydrogen in the film to adjust the mechanical properties of the film, it can meet different performance requirements (Ref 7, 21-24). Thus, hydrogen-free diamond-like carbon (DLC) and hydrogenated diamond-like carbon (HDLC) films are two main categories, and the difference is related to the content of sp^3 hybrid bonds and hydrogen content in films (Ref 6).

Shaomiao Shi, State Key Laboratory of Solid Lubrication, Lanzhou Institute of Chemical Physics, Chinese Academy of Sciences, Lanzhou 730000, China; and School of Materials Science and Engineering, Lanzhou University of Technology, Lanzhou 730050, China; **Xubing Wei, Xia Li, Guangan Zhang,** and **Zhibin Lu**, State Key Laboratory of Solid Lubrication, Lanzhou Institute of Chemical Physics, Chinese Academy of Sciences, Lanzhou 730000, China; **Qinglin Li** and **Chenglong Fan**, School of Materials Science and Engineering, Lanzhou University of Technology, Lanzhou 730050, China; **Shiyan Ding**, Key Laboratory of Advanced Technologies of Materials, Tribology Research Institute, Ministry Education, Southwest Jiaotong University, Chengdu 610031, China. Contact e-mails: lixia_090322@licp.cas.cn, liql301@mail.nwpu.edu.cn, gazhang@licp.cas.cn.

Diamond-like carbon films provide cost-effective solutions for various problems of manufacturing in industrial applications, such as improving properties and prolonging life of machine-components that are exposed to repetitive dynamic loading under extreme frictional contact conditions (Ref 16-18, 25-27). Hence, the performance evaluation and analysis by using reproducible and real-time dynamic response methods are critical for industrial applications of film (Ref 25, 28, 29).

However, there is the complex multi-factor phenomenon occurring during cyclic dynamic load damage, including cracks initiation, fracture, plastic damage behavior and chipping (Ref 30-32). And the superimposed of multi-factor will lead to the failure mechanism analysis of the film to be more complicated. Therefore, there are a few of studies on the impact wear behavior of protective film materials. In such case, a normal test of ball-to-flat contact impact that can obtain dynamic responses is a suitable alternative. The low velocity impact contact in this test more realistically reflects the impact wear resistance of film-substrate system under loaded intermittent contact and the evolution of impact wear under these conditions, compared to the impact test that simply controls the impact force.

Previous researchers were mostly limited to the impact resistance research of film materials (Ref 14, 15, 19, 33-35), and the effect of the substrate on the impact resistance under dynamic loading has been little studied. In addition, the research on the impact resistance of the film is mostly carried out from the perspective of changing the impact test parameters (such as impact force and impact frequency), but there is little research on the impact resistance of the film from the perspective of impact energy. In our previous work (Ref 36), we studied the impact wear resistance of DLC, HDLC and WC HDLC films on H62, and found that the impact resistance of the film was strongly depended on the hardness of the substrate. Therefore, we have compared the impact failure of films on different substrates to further explore the role of the substrate under the impact dynamic loads damage in this article. DLC, HDLC and WC HDLC films were deposited on GCr15 and

Published online: 17 March 2022

H62 substrates, respectively. Then a low velocity impact test based on the impact kinetic energy *Ei* control was performed on six film-substrate systems and substrates (GCr15 and H62). This test apparatus can obtain the impact force and impact contact duration in real time during the impact process. Then, these friction results of films and substrates were compared after impact load damage test. The reliability, durability and impact wear resistance of films under different film-substrate, same impact times and kinetic energy conditions were studied.

2. Experimental Method

2.1 The Film Preparation

Diamond-like carbon films (DLC and HDLC) were deposited by the unbalanced magnetron sputtering system (UPD650-4, Teer, England). Magnetron sputtering system combined with PECVD technology (Flexicoat 850, Hauzer Techno Coatings Ltd) was used to deposit WC HDLC films. The WC HDLC film had a three-layer structure consisting of a top HDLC films layer, a WC transition layer, and a very thin Cr bonding layer. Here, H62 and GCr15 steels (30 × 30 × 2 mm) polished to an average roughness Ra ≤ 0.2 μm were used as the substrate. Pure graphite targets (purity 99.99%) were used to obtain DLC and HDLC films. In the deposition process of WC HDLC film, C_2H_2 gas (purity 99.95%) was used as carbon source. However, in both deposition systems, Cr targets were used to deposit Cr interlayer to improve the adhesion strength. The details of the deposition process had been described in our previous paper (Ref 36). The specific deposition parameters of the films are shown in Table 1. The thickness of three kinds of deposited films is 2.5 ± 0.3 μm.

2.2 Mechanical Property Test

The hardness and elastic modulus of the films were determined by nano-indentation apparatus (TTX-NHT2, Anton Paar, Switzerland), which equipped with Berkvoich diamond indenter ($\alpha = 65.3° \pm 0.3°$ 2 μm). The nanoindentation device used the Oliver-Pharr calculation model. The load of nanoindentation test was loaded from 0 to a peak load of 10 mN at a loading rate of 20 mN/min and held for a 10 s residence time under peak load. The indentation depth was less than 1/10 of the film thickness, which had reduced the influence of underlying layer. The DLC, HDLC and WC HDLC films were measured 10 times to obtain the hardness of the films. The ratios of H/E and H^3/E^2 were calculated, which could be used as proxies of film fracture toughness and elastic strain resistance (Ref 37). In addition, the elastic recovery rate ($ER\%$) of the films was also calculated by using formula (1) and the load-displacement curves (Fig. 1) to estimate the elasticity of the films (Ref 9, 38).

$$ER = \frac{D_{\max} - D_{\text{res}}}{D_{\max}} \quad \text{(Eq 1)}$$

$D_{\max}$ is the maximum depth under the maximum load, and D_{res} is the residual depth after unloading.

The adhesive force of the films was determined by the scratch test. The scratch tester (RST3, Anton Paar, Switzerland) was equipped with a spherical diamond probe of 200 μm. The test was performed at a loading rate of 30 N/min, with a maximum load of 30 N and a scratch length of 5 mm. The adhesive force of the films was the critical load value for continuous peeling of the films.

2.3 Impact Tests

A reproducible and low velocity impact test method was used to evaluate the impact resistance of the films and substrates. The low velocity impact test apparatus had been introduced in detail in our previous work (Ref 36). The control method of the low-velocity impact tester was based on the impact kinetic energy *Ei* instead of the impact force. Here, the impact energy *Ei* was determined by the impact velocity *vi* and the impact mass *m*. The counterpart was adopted GCr15 hard steel sphere with diameter of 10 mm. The low velocity impact test was conducted at room temperature (temperature and humidity are 25 °C and 60%RH, respectively). Before the test, all of the films, substrates and the impactors were cleaned with anhydrous ethanol and dried. In all tests, the velocity of the impact ball vi = 80 mm/s and the impact mass m = 100 g to ensure that the same impact energy was applied to each film-substrate system. Each sample was impacted 10,000 times, and every film was repeatedly tested three times to ensure reliability of data.

The morphology of the impact craters was measured by the field emission scanning electron microscope (FESEM, TESCAN, MIRA3) under the condition of an accelerating voltage of 10 kV and a Probe current 5 μA. Chemical compositions of the impact craters composite coatings were characterized by an energy-dispersive spectroscopy (EDS). The analysis of the components and structures of the impact craters films was performed using confocal Raman spectrometer (Jobin-Yvon LabRAM HR Evolution, France).

Table 1 Deposition parameters of films

	DLC	HDLC	WC HDLC
Deposition method	Unbalanced magnetron sputtering	Unbalanced magnetron sputtering	Magnetron sputtering + PECVD
Working pressure, Pa	6.4	6.4	3.0×10^{-3}
Bias voltage, V	70	70	660V
Target current, A	3.5	3.5	…
Gas flow, sccm	…	C_4H_{10} (16)	C_2H_2 (300)

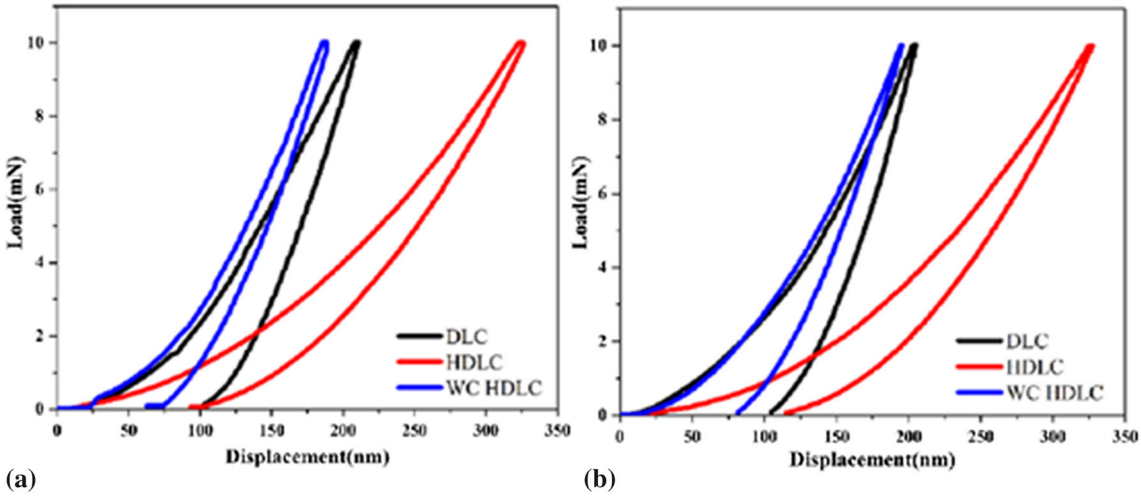

Fig. 1 Load-displacement curve of films. (a) films on H62, (b) films on GCr15

Table 2 Element content of H62 and GCr15 substrates

Substrates	Chemical composition, wt.%				
H62	Cu	Zn	Fe	Sb	P
	61.50	38.30	0.14	0.05	0.06
GCr15	Fe	C	Cr	Si	Mn
	Bal.	0.95-1.05	1.40-1.65	0.15-0.35	0.25-0.45

3. Results and Discussion

3.1 Characterization of Films

The chemical element content of the H62 and GCr15 substrates is listed in Table 2 through EDX analysis, and the total element composition is normalized to 100 wt.%. The hardness (H), elastic modulus (E), and other mechanical properties parameters of films on GCr15 are listed in Table 3. However, the mechanical properties of the films on H62 are the same as results of our previous work, as shown in Table 4. The type of substrate basically has no effect on the hardness (H) and elastic modulus (E) of the corresponding films. However, the adhesion force of the deposited films is affected and increases as the substrate hardness improves. This is because of the reduction in the difference in thermal expansion coefficient and the mismatch degree between the films and substrates (Ref 39, 40). The ratios of H/E and H^3/E^2 are less pronounced different in the films on GCr15 and H62. It can also be seen that the elastic recovery rate ($ER\%$) of HDLC and WC HDLC films is higher than that of DLC, which shows that the elasticity of HDLC films is greater than that of DLC. Figure 2 shows a cross-sectional SEM image of the deposited films. The Cr bonding layer and the WC transition layer can be clearly observed between the deposited film and the substrate. And it is tightly combined with the films and the substrate without obvious defects. In addition, DLC, HDLC and WC HDLC films all exhibit a dense microstructure, which also indicates that the films were successfully prepared.

3.2 Scratch Test

Adhesive and cohesive failure modes of films as well as the load bearing capacity of film-substrate system can be elucidated through the scratch test (Ref 30, 37). The scratch tracks and the curve of scratch depth of GCr15 and H62 film-substrate systems are presented in Fig. 3 and 4. The minimum load of cracking occurs (cohesive failure) is called L_{c1}, and the load of the film beginning to peel off continuously (adhesive failure) is called L_{c2}.

It is shown in Table 3 and Fig. 3 that the critical loads of cohesive failure of the DLC, HDLC and WC HDLC films on GCr15 subtract are 4.5, 8.1 and 10.9 N, respectively. The critical loads of adhesive failure of these three different films are 10.3, 19.6 and 19.6 N, respectively. It can be inferred that the WC HDLC film on GCr15 possessed more superior crack initiation resistance and adhesive failure resistance than that of the DLC and HDLC on GCr15. However, it is shown in Table 4 and Fig. 4 that the critical loads of cohesive failure of DLC, HDLC and WC HDLC films on H62 are 3.2, 1.2 and 2.9 N, respectively, and the critical loads for adhesive failure are 8.3, 12.1 and 11.8 N, respectively. The films on H62 have poorer crack initiation resistance and adhesive failure resistance compared with the films on GCr15. The various curve of scratch depth shows that WC HDLC on GCr15 has almost no change in scratch depth. This indicates that WC HDLC film-substrate system on GCr15 possessed higher load bearing capacity, and potentially superior impact resistance. In addition, the varies curve of scratch depth shows that the film-substrate system on H62 possessed similar scratch depths. And its scratch depth is greater than the films on GCr15. Hence, the result indicates that the capacity of load bearing of the film-substrate system on H62 is the worst.

The cohesive failure started to appear after the sliding stage. Cohesion cracks were mainly caused by the superposition of intrinsic stress inside the film material, the shear stress and tensile stress during the scratch tests, which eventually leaded to the fracture of film (Ref 14). However, the adhesive failure started to appear as the load continued to increase. The external stress and interface mismatch stress were main reasons for their peeling and decreased durability (Ref 41, 42).

Table 3 Mechanical properties of the films on H62

	Hardness, GPa	Elastic modulus, GPa	*H/E*	H^3/E^2	*RE*, %	Adhesion force, N
DLC	15.9 ± 0.4	178.1 ± 1.2	0.09	0.13	52.0	8.30 ± 0.1
HDLC	7.1 ± 0.3	59.7 ± 1.5	0.12	0.10	71.3	12.10 ± 0.4
WC HDLC	23.8 ± 0.8	188.1 ± 12.3	0.13	0.38	66.7	11.80 ± 0.9
H62	3.2 ± 3.0	144.9 ± 5.0	…	…	…	…

Table 4 Mechanical properties of the films on GCr15

	Hardness, GPa	Elastic modulus, GPa	*H/E*	H^3/E^2	*RE*, %	Adhesion force, N
DLC	17.0 ± 0.9	205.1 ± 5.6	0.08	0.12	48.8	10.3 ± 1.6
HDLC	7.3 ± 0.2	65.4 ± 3.4	0.11	0.09	64.6	19.6 ± 1.1
WC HDLC	21.0 ± 3.3	194.0 ± 22.9	0.11	0.25	58.4	19.6 ± 0.4
GCr15	9.7 ± 0.4	257.8 ± 5.3	…	…	…	…

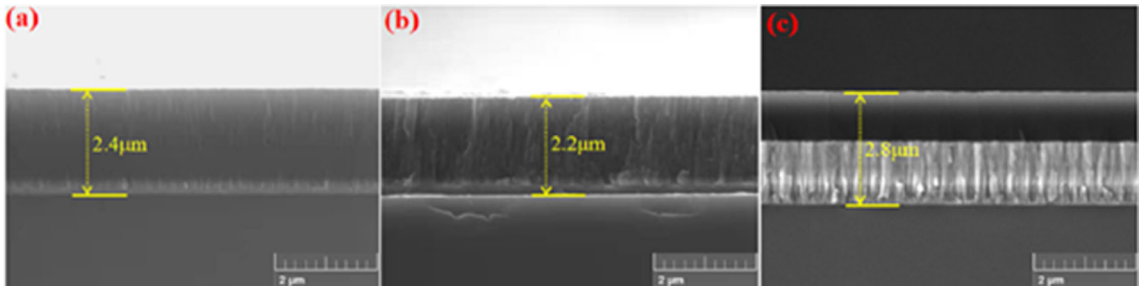

Fig. 2 Cross-sectional SEM image of the deposited films (a) DLC, (b) HDLC, (c) WC HDLC

3.3 Impact Tests Dynamic Response

Figure 5 shows that the nonlinear variation trend of impact force that is controlled by impact kinetic energy. It should be noted that the impact force represents a test result rather than a parameter. The results of waveform curve of impact force indicated that the types of substrate had significant influence on impact force F and impact contact duration t. It was obvious that the impact force on GCr15 was larger than H62, but the impact contact time was shorter. The impact contact duration t will affect the strain ratio. In addition, the impact force of the three different films on GCr15 is higher than that of the corresponding films on H62, and the impact contact time is also shorter, as shown in Fig. 5. This was considered to be caused by the difference hardness in the substrate. The three different films on H62 was prone to release the impact energy through elastoplastic deformation of the soft substrate, so that the impact force was reduced. However, the three different films on hard GCr15 substrate were not easy to release impact energy. Hence, the impact force was relatively large in the impact process.

In addition, the WC HDLC film on H62 had a higher impact force then DLC and HDLC film on H62, which was attributed to the existence of WC interlayer. The existence of WC could improve the hardness and adhesion of the film (Table 3), but the WC interlayer reduced the elastoplastic deform-ability of the film-substrate system. Hence, the impact force F on WC HDLC film on H62 was obviously larger. Besides, it was found from Table 3 and Fig. 5 that the impact force of film-substrate systems on H62 increased with the increase in film hardness. However, the impact force of the film-substrate systems on hard GCr15 did not change significantly. This was believed to be caused by the hard GCr15 substrate that was not prone to deform and could play a good role in supporting the film.

3.4 Raman Analysis

Figure 6 shows the variation in the I_D/I_G ratio, FWHM and G-peak position of the Raman spectrum of the films surface and the impact craters. The G peak did not shift to a high frequency, and I_D/I_G ratio at different positions was not much different, indicating that the sp^3-sp^2 phase transition was not obvious on the impact craters for the three films on GCr15 after impacting. No graphitization of films on GCr15 occurred during the test, and the change in FWHM was less pronounced. This is due to the GCr15 steel substrate could play a good supporting role to films, and the films basically did not undergo bending deformation during the impact process. Hence, no shear stress and bending stress generated in the films impact test. In addition, the heat generated during the impact test did not cause graphitization of the films on GCr15.

However, the graphitization of the films on H62 was particularly obvious (Ref 36), and the G-peak shifted to the high frequency, and the I_D/I_G ratio increases, especially at the B position. This were considered to be caused by the combined

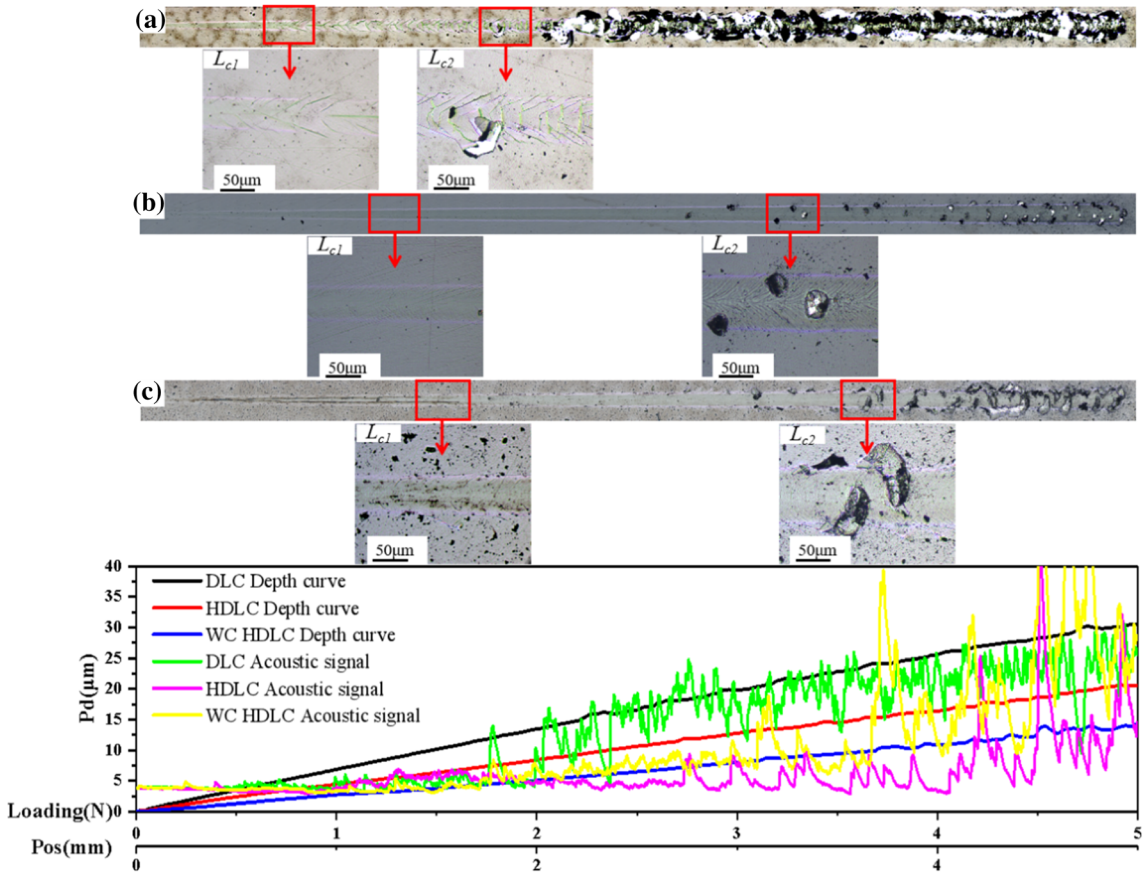

Fig. 3 The scratch tracks and the depth curve of films on GC15 (a) DLC, (b) HDLC, (c) WC HDLC

effect of heat generated during the impact test, bending stress and shear stress.

3.5 Morphological Analysis

After the test, 3D surface morphology and cross-sectional profile of the impact craters were shown in Fig. 7 and 8. It was obvious that the depth of the impact craters on the H62 and GCr15 substrates was significantly greater than that of all the diamond-like carbon film samples, except for the WC HDLC on the H62. Meanwhile, bulges were observed along the edge of wear craters. Therefore, DLC and HDLC films can provide protection to its substrate and make it have better impact resistance, no matter the GCr15 substrate or H62 substrate. The result indicates that the WC HDLC film on H62 possesses the largest wear profile (width $\geq$ 500 μm and depth $\geq$ 6 μm), and leads to large plastic deformation of the substrate. In three different films on GCr15, impact craters of DLC and HDLC films have the larger depth than that of WC HDLC film (Fig. 8a), which means that the WC HDLC film on GCr15 possesses superior impact resistance. But anyway, the depth of impact crater of three different films on GCr15 are smaller ($\leq$ 0.2 μm) compared to three films on H62 (Fig. 8b), which means that the impact cyclic dynamic load does not cause plastic deformation of the GCr15 steel substrate.

In contrast, the width ($>$ 348 μm) and depth ($>$ 1.7 μm,) of the impact craters of three films on H62 are larger (Fig. 8b). In the previous reports (Ref 28), the failure forms of film-substrate system are mainly composed of interface wear and plastic deformation, during the impact process. As evident from Fig. 7 and 8, the hard substrate can not only improve the adhesion of the films (Table 3 and 4), but also play a good supporting role for the films, in avoiding plastic deformation of the substrate under dynamic impact load.

The SEM images of H62 and GCr15 are illustrated in Fig. 9 and 10. The oxygen element on the surface of the impact crater increased, indicating that friction oxidation occurred and a large area of white oxide layer appeared during the impact process. Meanwhile, the oxidized white layer began to delaminate and peel off under the cyclic dynamic load. In addition, there was only a small amount of white oxide layer inside the impact craters. But severe wear occurred at the edge of the impact craters, and a large amount of white oxide layer was accumulated, which was caused by the occurrence of plastic deformation.

Figure 10 shows the SEM morphology of DLC film on GCr15. It was apparent that a number of tiny, local fatigue cracks formed and distributed irregularly inside the impact crater. However, there was no significant failure along the rim of craters. These were considered to be caused by the larger contact stress at the local positions of the impact crater. In addition, shear stress and bending stress were also generated under cyclic dynamic damage. Eventually, the synergistic effect of three stresses led to the initiation of cohesive cracks (no fracture), but it did not cause the adhesive failure, such as spalling.

In contrast, in our previous study, we found that the DLC film on H62 had less failure inside the impact crater, but fracture and spalling occurred at the rim of the impact crater

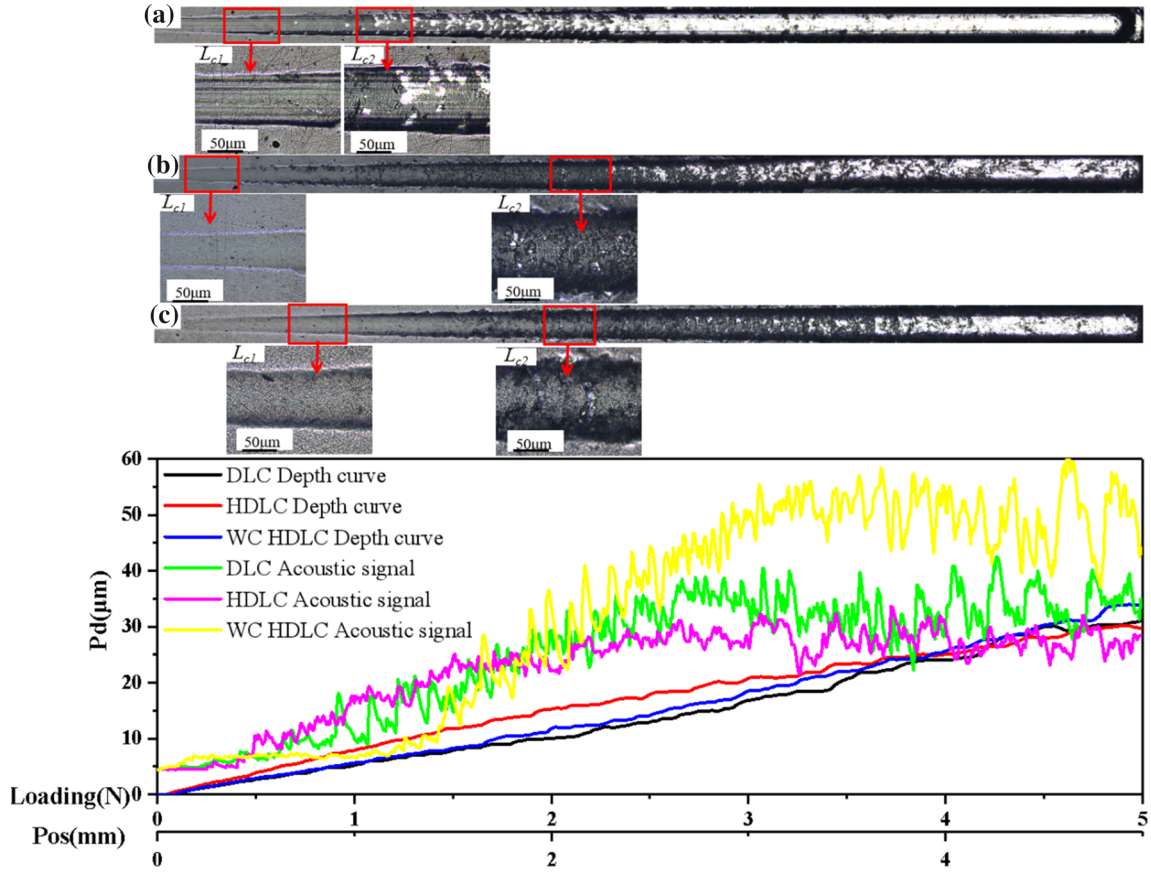

Fig. 4 The scratch tracks and the depth curve of films on H62 (a) DLC, (b) HDLC, (c) WC HDLC

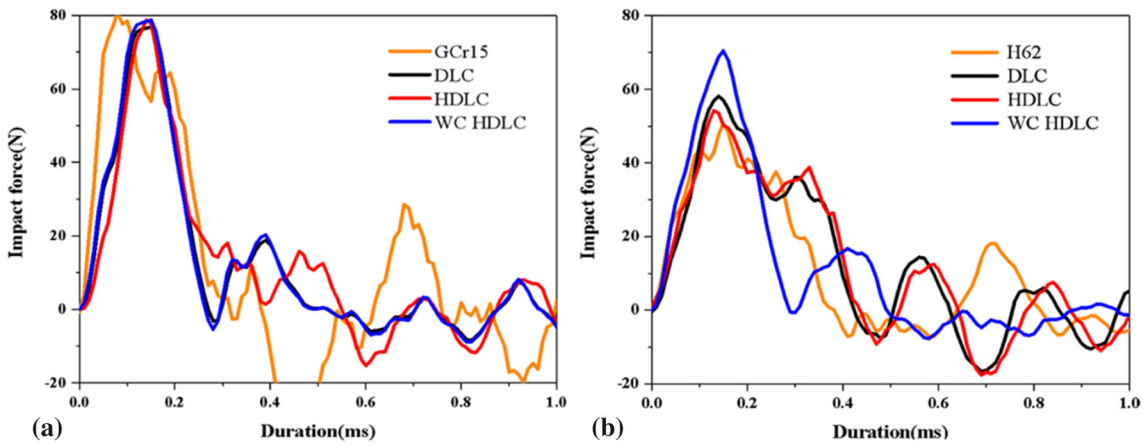

Fig. 5 Waveform curve of impact force (a) films on GCr15, (b) films on H62

(Ref 36). The difference of the failure mechanism for the DLC film can be attributed to enhance the substrate hardness. Because the higher hardness of the film-substrate system on GCr15 steel is less prone to plastic deformation, which makes it difficult for the counterpart ball and the flat plate to transfer from point contact to surface contact. In this case, it will cause serious failure inside the impact crater.

In addition, previous studies had confirmed that there was a large tensile stress in the rim of the impact crater (Ref 14, 29). However, the adhesion force of the film-substrate systems on GCr15 increased with the film hardness (Table 3 and 4). Hence, the tensile stress at the rim of the impact crater was insufficient to cause the DLC film on GCr15 to fail. The result of EDX showed that the Fe and O elements at the DLC interface were increased after suffering cyclic dynamic damage, which resulted in a corresponding decrease in carbon intensity, especially at the rim of the impact crater. The result indicated that material transfer occurred at the contact interface and iron was oxidized (Fig. 11).

After the impact test, the white oxide layer appeared at the rim of the impact crater of the HDLC film on GCr15, as shown in Fig. 12. However, the impact dynamic load caused neither

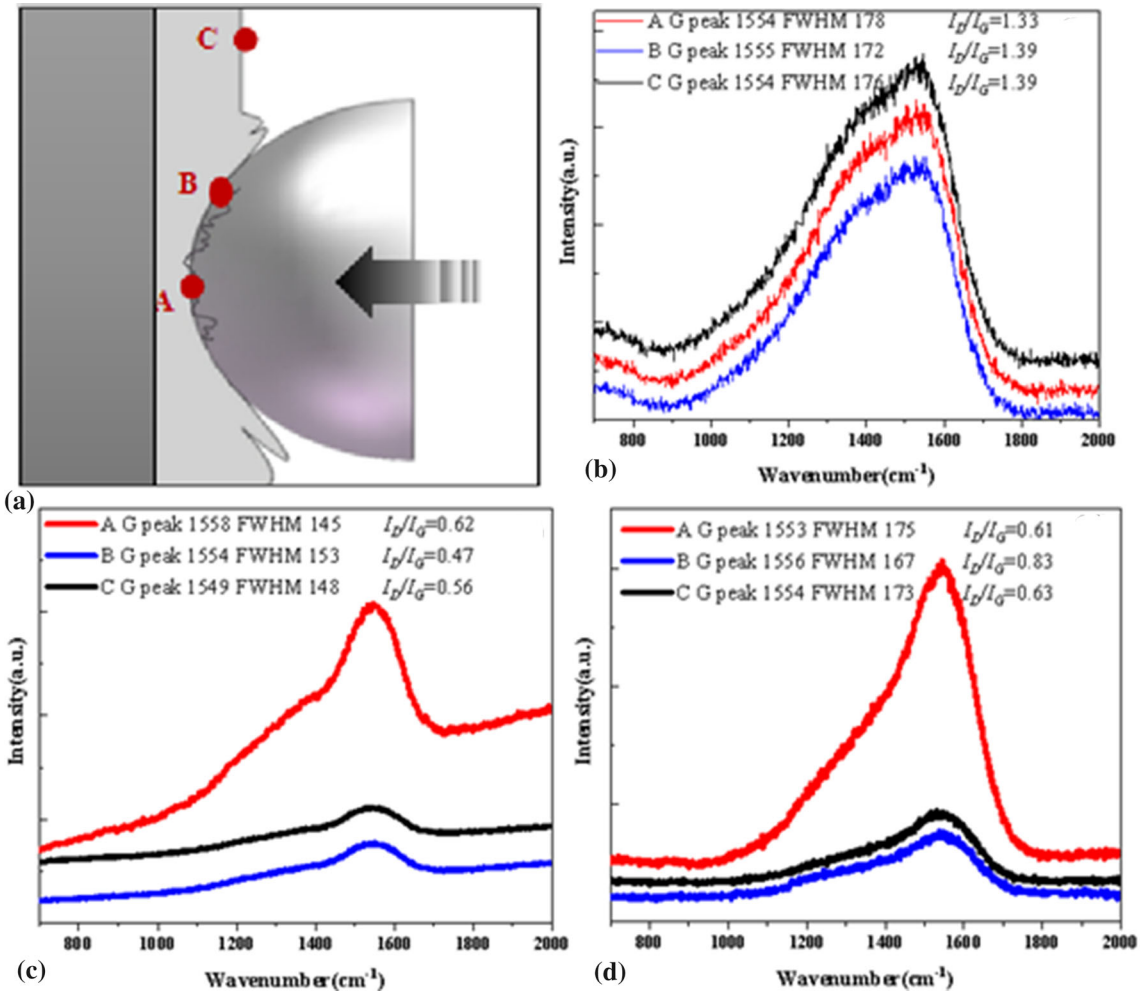

Fig. 6 (a) Raman spectra detecting locations of GCr15 films, (b) DLC, (c) HDLC, (d) WC HDLC

the cohesive failure nor the adhesive failure. It indicates that the HDLC film on GCr15 has the best impact resistance. This speculation can be confirmed by the 3D surface morphology and cross-sectional profile analysis in Fig. 7 and 8. Compared with HDLC on GCr15, although HDLC on H62 underwent severe plastic deformation under dynamic impact load, it did not fail significantly (Ref 36). It is believed that this is due to the lower hardness, higher *ER%* and good adhesion of the HDLC film (Table 3 and 4).

Therefore, it can be seen that regardless of the hardness of the substrate, the synergistic effect of the low hardness, higher *ER%* and high adhesion of the film can obviously prevent the failure of the film. The EDX of HDLC results show that the white transfer layers at the rim of the impact crater are mainly oxygen and iron.

Figure 13 presents the SEM image of WC HDLC film on GCr15. No failure appeared in the central area of the impact crater, but the adhesive failure occurred at the rim of the impact crater, after the impact test. This can be attributed to the higher bearing capacity of the film-substrate system (Fig. 3). Hence, the impact compressive stress cannot lead to failure of the film in the compressive stress area. This speculation can be confirmed by the curve of scratch depth analysis and cross-sectional profile in Fig. 3 and 8. However, due to the accumulation of tensile stress on the rim of the impact crater, the film eventually peels off. Numerous studies have found that the stress distribution of ball-plate contact according to Hertz contact theory (Ref 14, 29), which also confirms that the area in contact with the counterpart ball is the compressive stress area, and at the rim of the impact crater is the tensile stress area.

In addition, it is shown in Fig. 8 that the WC HDLC film on GCr15 was basically not deformed under cyclic dynamic load, which resulted in a small contact wear area between the ball-plate. Thus, the interface wear between the ball-plate was very small. Eventually, the impact crater of the WC HDLC film on GCr15 did not undergo material transfer after the cyclic impact test. And the EDX analysis results of the impact crater of the WC HDLC film on GCr15 show that almost no Fe transfer or tribo-oxidation can be detected during the cyclic impact wear test.

However, it could be seen from previous studies that the WC HDLC film on H62 had significant failure after the impact test (Ref 36), and the film peeled off over a large area inside and around the impact crater. This was because H62 substrate could not play a good supporting role for the film when it was subjected to cyclic dynamic load, which led to the WC interlayer fracture. Eventually, the WC HDLC film collapsed. By analyzing the test results of the films on the two types substrates (GCr15 and H62), it can be clearly found that hard substrate can not only improves the adhesion force (Table 3 and

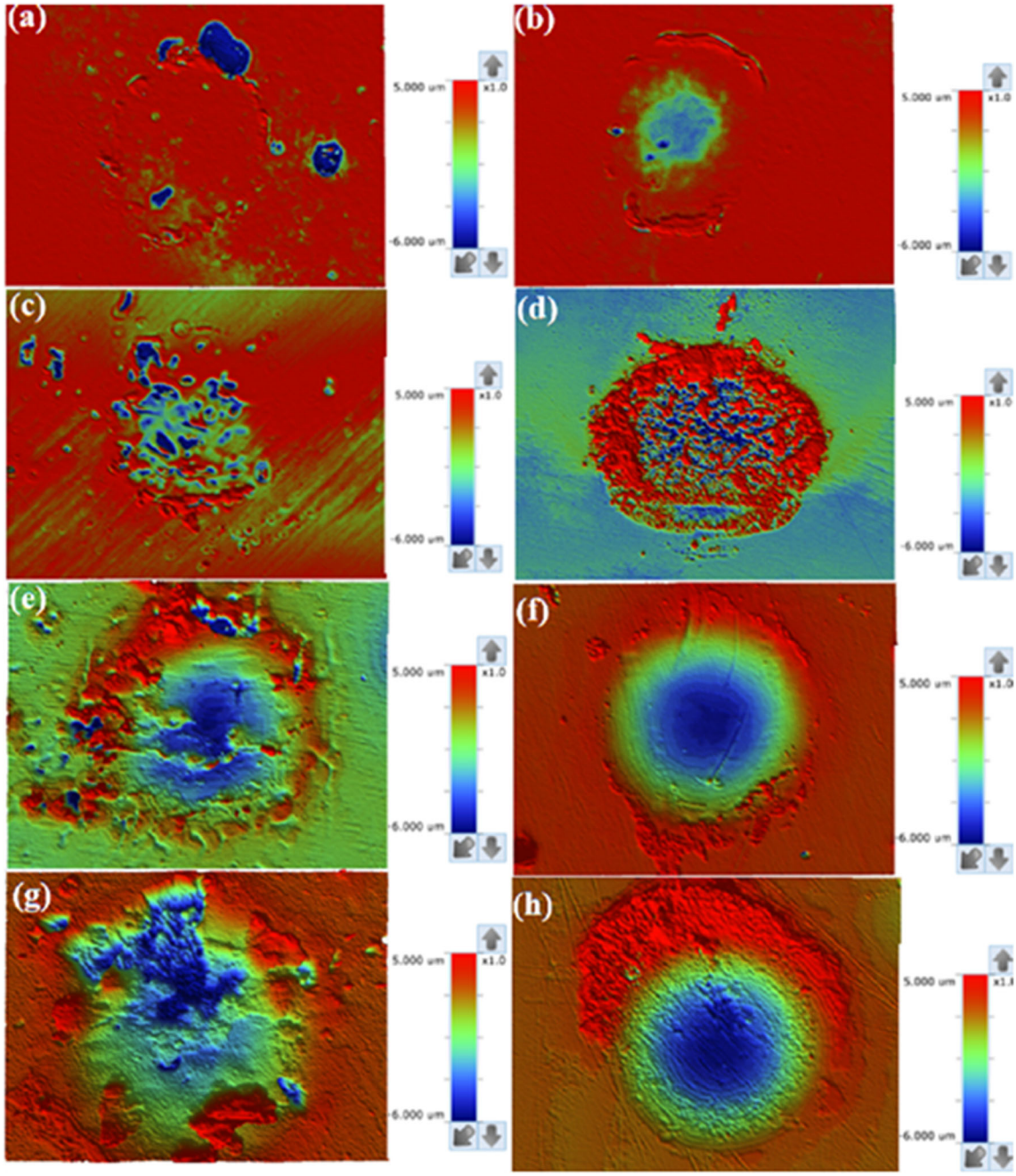

Fig. 7 The 3D surface morphology of impact craters on GCr15 (a) DLC, (b) HDLC, (c) WC HDLC, (d) GCr15; impact craters on H62 (e) DLC, (f) HDLC, (g) WC HDLC, (h) H62

4), but also can play a good supporting role for film during the cyclic impact. Thus, it is important for a given tribological application to choose the appropriate film-substrate system.

Tan et al. (Ref 15) used PVD technology to obtain WC DLC film, the elastic modulus and nanoindentation hardness of which were 76.2 ± 22 and 15.3 ± 2.1 (GPa), respectively. Chen et al. (Ref 19) used the PACVD deposition technique to deposit the WC DLC film, the hardness and elastic modulus of which were 20.5 and 180 GPa, respectively. Hee et al. (Ref 20) used a hybrid magnetron sputtering method to deposit HDLC in a deposition chamber equipped with integrated arc and multi-target magnetron sputtering technology (Milman Hybrid Deco-coater). The hardness and elastic modulus of HDLC were, respectively, 16.5 ± 0.66 and 124 ± 3.63 (GPa). Wang et al. (Ref 43) deposited HDLC on 304 stainless steel through an unbalanced magnetron sputtering system (Teer UDP-650). Its hardness and elastic modulus values were 7.5 ± 0.2 and 72.6 ± 1.7 (GPa), respectively. Sutton et al. (Ref 44) used PECVD deposition technology to obtain HDLC films at extremely low temperatures, with hardness and elastic modulus values of 21.3 and 191 GPa, respectively. Maruno et al. (Ref 9) used PECVD technology to deposit DLC film on A2024 aluminum alloy substrate. The hardness and elastic modulus were 19.9±4.5 and 196 ± 30 (GPa), respectively. The film hardness and elastic modulus values obtained in this paper are not much different from those obtained by other authors' work

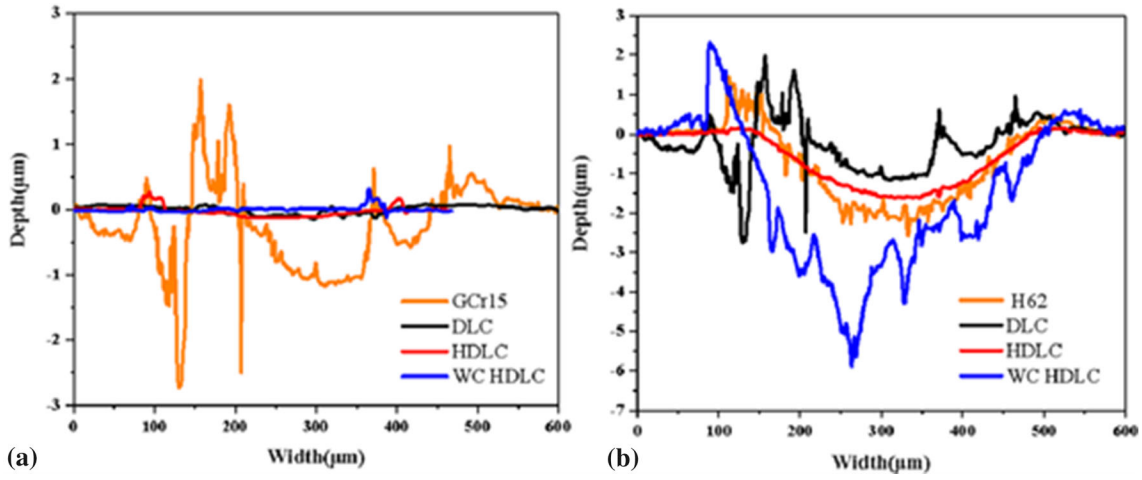

Fig. 8 The 3D cross-sectional profile (a) films on GCr15, (b) films on H62

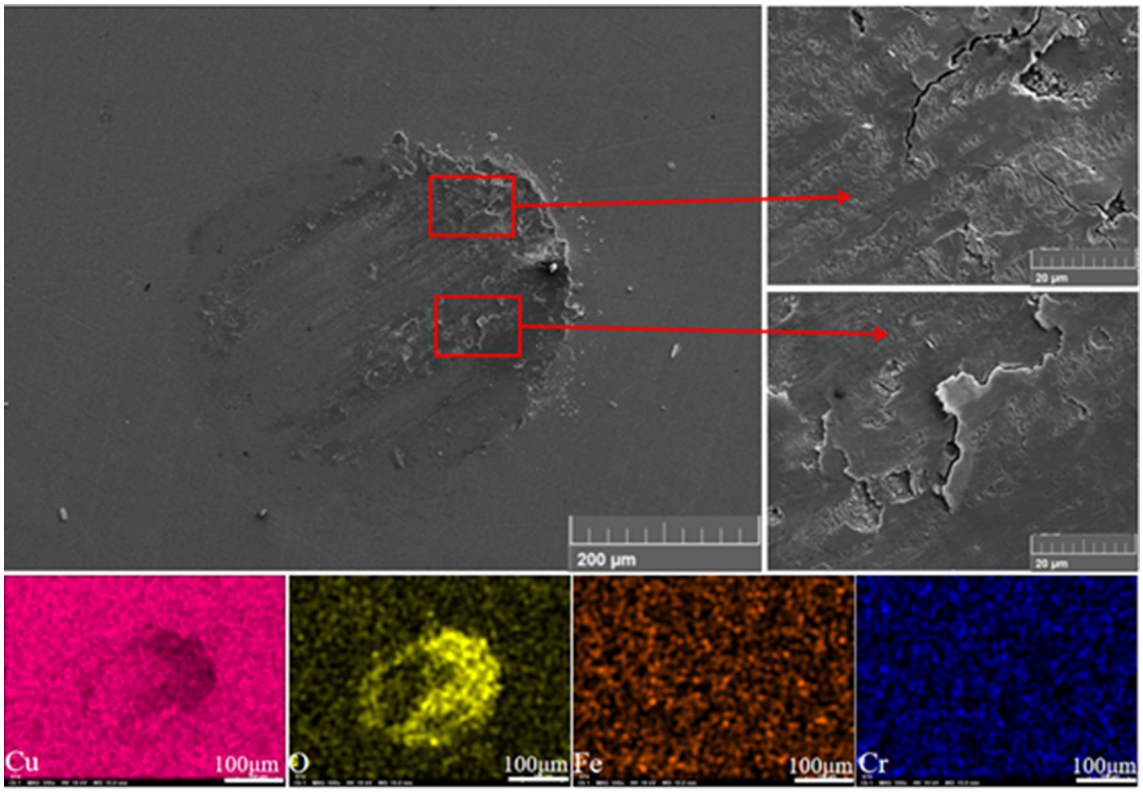

Fig. 9 The SEM morphology of H62

on DLC and HDLC films. When the transition from elastic behavior to fracture strength of the film material is narrow (that is, almost no plastic deformation), this means that the brittleness of the film material is high. Under cyclic dynamic impact loading, the fatigue effect easily leads to the failure of the brittle film. Obviously, if the local strain is lower than the strain corresponding to the yield stress of the film, no fatigue effect will occur. Therefore, in order to improve the failure resistance of film materials under impact load, it is necessary to choose film materials with low hardness and high elastic modulus. In addition, it is shown in Table 3 and 4 that the elastic recovery (*ER%*) of HDLC is excellent regardless of whether the substrate is hard or soft. Studies have shown that a higher *ER%* indicates that films possess greater elasticity (Ref 38). In addition, according to the researches of Sam Zhang et al. (Ref 45), the load-displacement curve can be divided into an elastic deformation stage and a plastic deformation stage. It can be seen from the load-displacement curve of HDLC (Fig. 1) that the plastic deformation of HDLC is the most serious the indentation load. However, due to low hardness, higher *ER%* and high adhesion of HDLC film. Hence, there is no obvious failure under impact load. In contrast, the plastic deformation of DLC and WC HDLC is smaller in the load-displacement curves, but because the low adhesion force and the existence of the WC interlayer. Therefore, the failure is more serious than HDLC. Besides, because the HDLC film is softer, it has lower

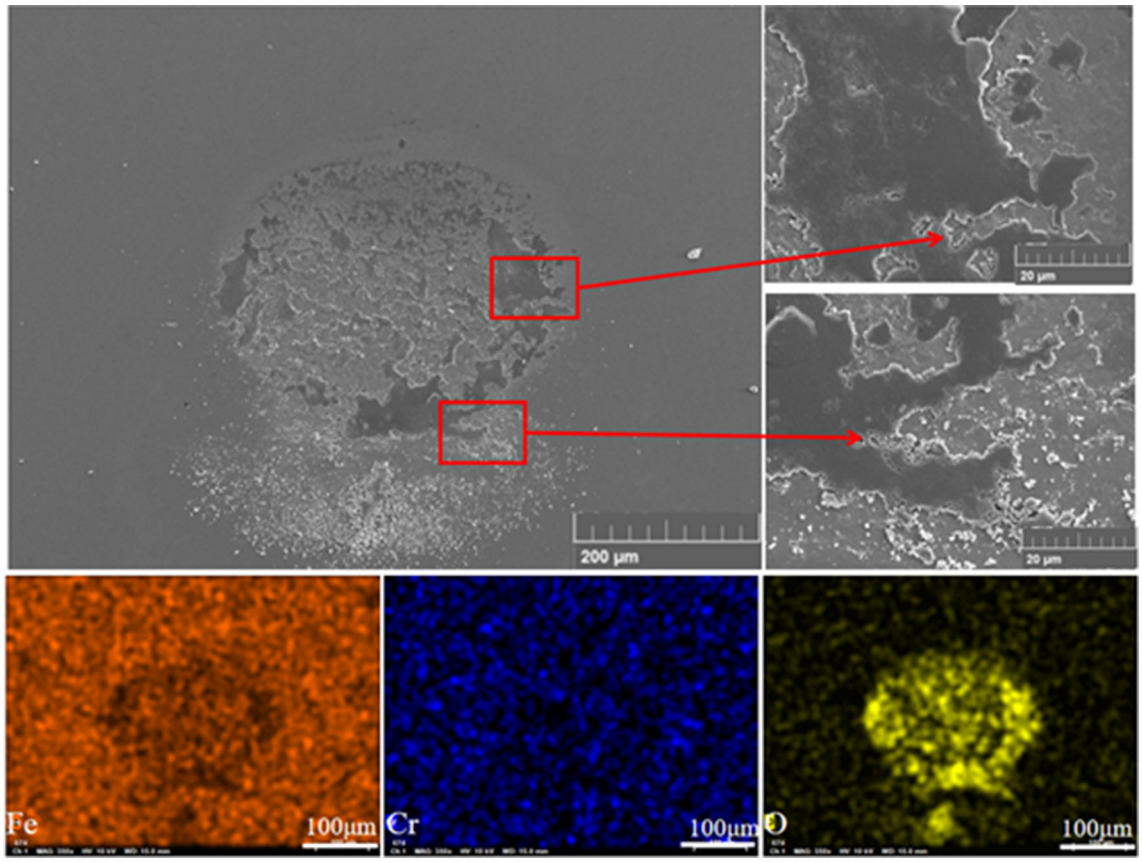

Fig. 10 The SEM morphology of GCr15

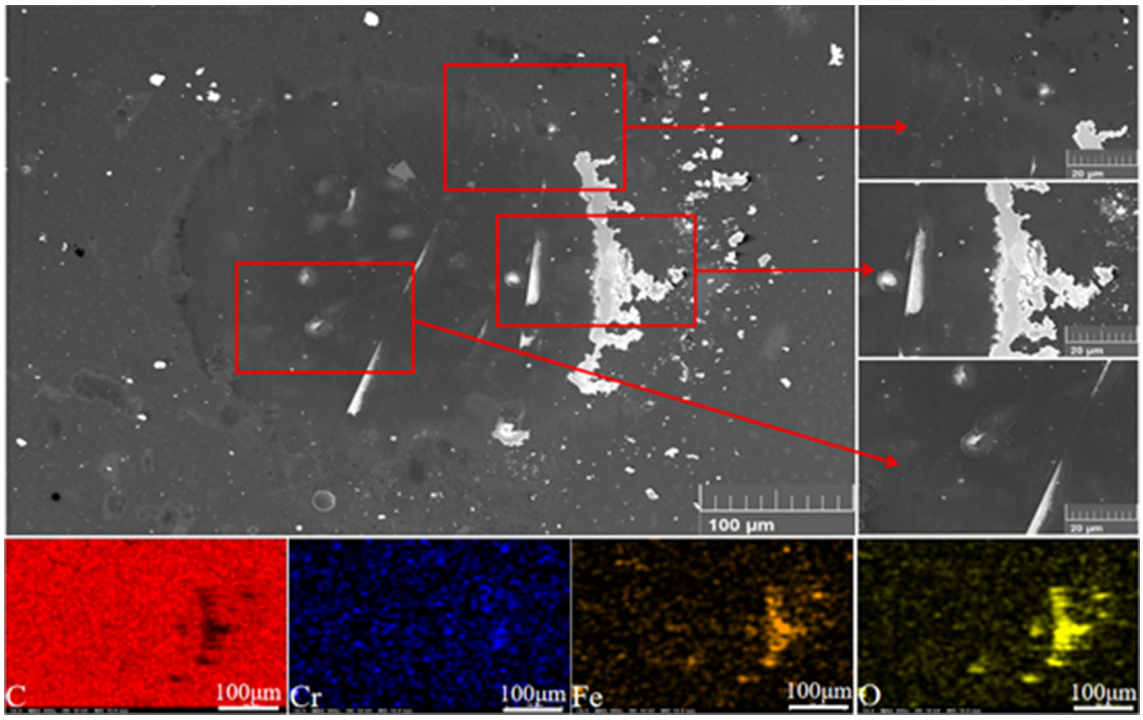

Fig. 11 The SEM morphology of DLC film on GCr15

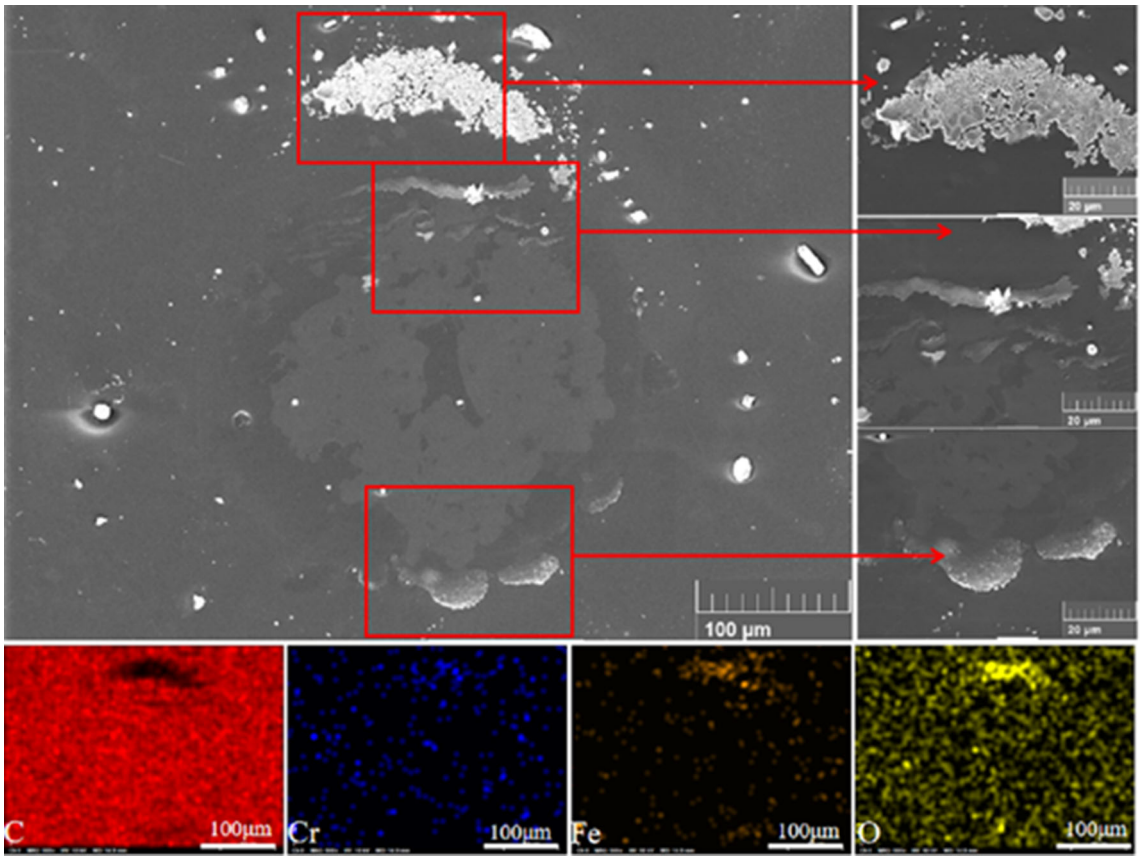

Fig. 12 The SEM morphology of HDLC film on GCr15

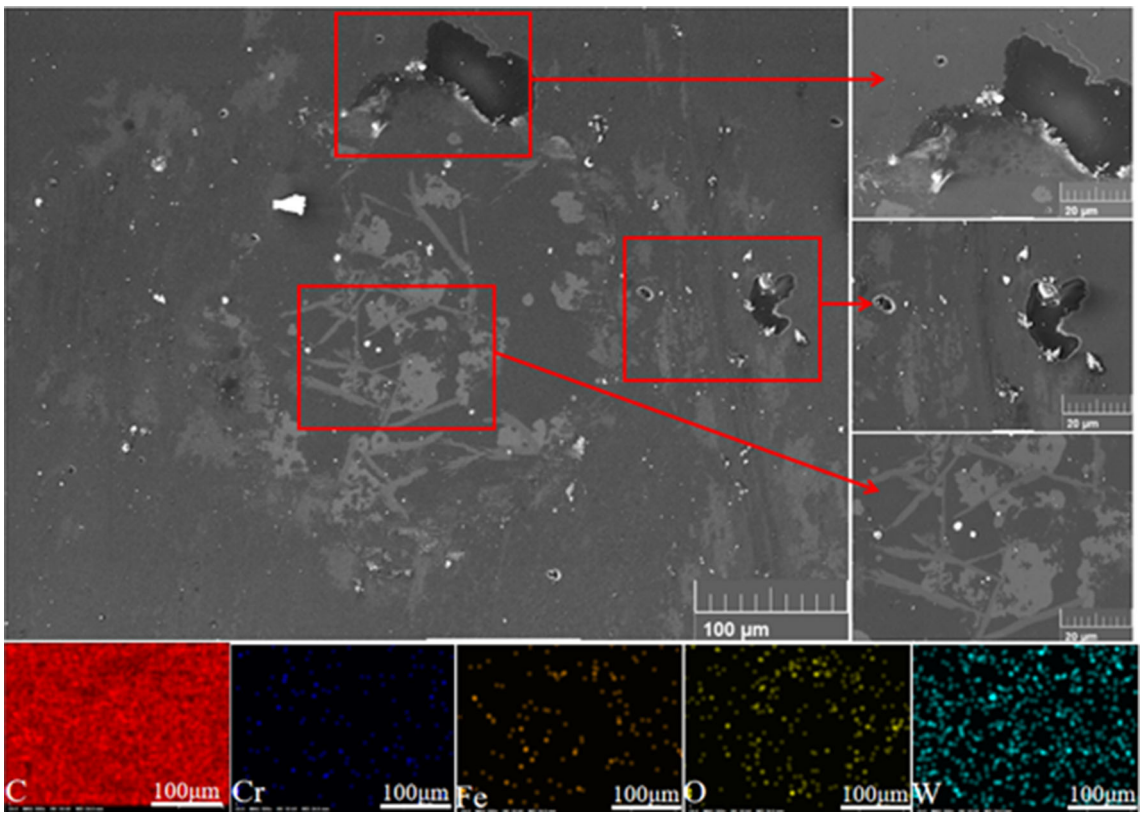

Fig. 13 The SEM morphology of WC HDLC film on GCr15

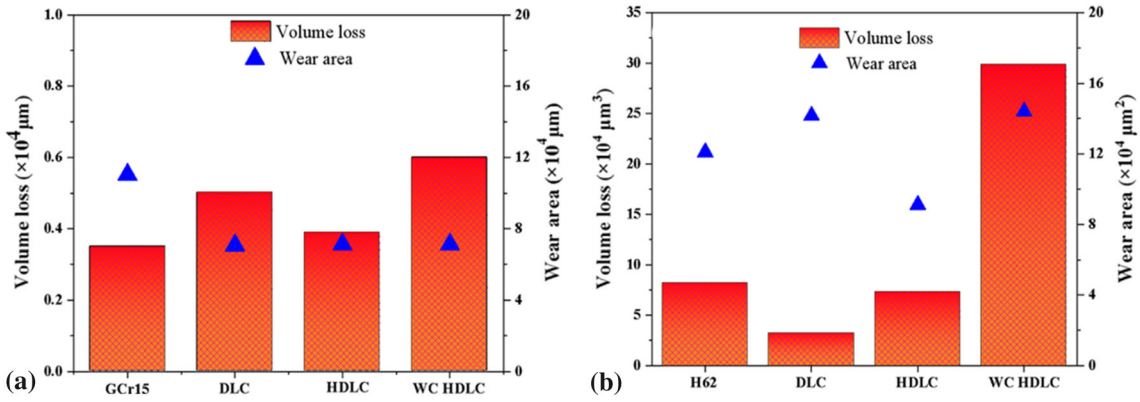

Fig.14 The volume loss and wear area (a) films on GCr15, (b) films on H62

internal stress and excellent ductility, which can relax the interface shear forces in the system (Ref 34, 35).

There is a certain correlation between the scratch test and the impact test. The scratch test results (Fig. 3 and 4) can clearly show that the film-substrate on the H62 undergoes a larger plastic deformation during the scratch test due to the normal load gradually increases. H62 cannot provide good support to the films, which leads to the main failure mechanism of the films is cohesive failure. However, the film-substrate on GCr15 does not undergo plastic deformation during the scratch test. When the load is gradually increased from 0 to 30 N, the GCr15 substrate can provide good support for the films. Therefore, the failure mechanism of the films on GCr15 is mainly adhesive failure. Compared with the scratch test, the film-substrate system is mainly subjected to normal load in the dynamic impact test, and there is no tangential force. In addition, the plastic deformation of the films will also increase the stress energy of the system. The plastic deformation of the films on GCr15 is smaller than that on H62, which indicates that the stress and energy of the films on GCr15 are smaller than that on H62. In addition, the adhesive strength of the films on GCr15 is greater than that of the films on H62, which indicates that the films on GCr15 has greater binding energy and lower interface mismatch stress. Therefore, the hardness of the substrate is particularly important under dynamic load, and it will indirectly affect the failure mechanism of the film. The film on the hard substrate is not prone to fracture. But on the soft substrate, the film is easy to fracture and peel off.

Figure 14 presents the volume loss and wear area of different film-substrate system. It is observed that the volume loss and wear area of the films on H62 are larger than that of GCr15. The result shows that it is clear that the hard substrate can effectively reduce the damage of the films material under impact dynamic load.

4. Conclusions

The DLC, HDLC and WC HDLC films on the GCr15 and H62 substrates were performed a low-speed impact test based on the impact kinetic energy *Ei* control. Then, the friction results of the film-substrate systems were compared and analyzed. Concluded as follow:

(1) Although the harder substrate causes a large impact force under the same impact energy (the impact force of the film on the hard substrate is greater than the film on the soft substrate), the hard substrate can provide a good support for the film when subjected to cyclic dynamic loads to avoid plastic deformation of the film-substrate system.

(2) The film-substrate system releases impact energy through elastoplastic deformation. Hence, it can reduce the impact force. In addition, the impact force on the soft substrate will increase with the increase in the film hardness under the same impact energy, but the hardness of the film on the hard substrate has little effect on the impact force.

(3) The high hardness and brittleness of the WC interlayer will reduce the impact resistance of the film on soft substrates, but it will have less effect on hard substrates.

(4) The synergistic effect of the low hardness, higher *ER%* and high adhesion of HDLC film, which makes it to possess superior impact resistance regardless of whether it is on a soft substrate or a hard substrate. Hence, among the six film-substrate systems tested, HDLC film is found to be the most suitable for applications involving impact dynamic loading.

Acknowledgments

The authors wish to acknowledge the financial support of the National Natural Science Foundation of China (Grant Nos. 11972344, 51775535), the State Key Laboratory of Solid Lubrication, Lanzhou Institute of Chemical Physics, Chinese Academy of Sciences, Lanzhou 730000, China.

References

1. K. Holmberg, and A. Erdemir, The Impact of Tribology on Energy use and CO_2 Emission Globally and in Combustion Engine and Electric Cars, *Tribol. Int.*, 2019, **135**, p 389–396.
2. S. Zhang, J. Liu, and Y. Zhou, Effect of DLC Coating on the Friction Power Loss Between Apex Seal and Housing in Small Wankel Rotary Engine, *Tribol. Int.*, 2019, **134**, p 365–371.
3. X. Chen, C. Zhang, T. Kato, X.A. Yang, S. Wu, R. Wang, M. Nosaka, and J. Luo, Evolution of Tribo-Induced Interfacial Nanostructures

Governing Superlubricity in a-C: H and a-C:H: Si Films, *Nat. Commun.*, 2017, **8**, p 1675.
4. S.D.A. Lawes, S.V. Hainsworth, and M.E. Fitzpatrick, Impact Wear Testing of Diamond-Like Carbon Films for Engine Valve-Tappet Surfaces, *Wear*, 2010, **268**, p 1303–1308.
5. A. Igartua, E. Berriozabal, R. Nevshupa, E. Roman, F. Pagano, L.P. Nielsen, S. Louring, and L. Muntada, Screening of Diamond-Like Carbon Coatings in Search of a Prospective Solid Lubricant Suitable for both Atmosphere and High Vacuum Applications, *Tribol. Int.*, 2017, **114**, p 192–200.
6. J. Wang, X. Li, G. Wu, Z. Lu, G. Zhang, and Q. Xue, Origin of Low Friction for Amorphous Carbon Films with Different Hydrogen Content in Nitrogen Atmosphere, *Tribol. Int.*, 2019, **140**, p 105853.
7. A. Erdemir, and C. Donnet, Tribology of Diamond-Like Carbon Films: Recent Progress and Future Prospects, *J. Phys. D. Appl. Phys.*, 2006, **39**, p 311–327.
8. Y. Uematsu, T. Kakiuchi, M. Adachi, and T. Shinohara, Effect of Interlayer Thickness on Fatigue Behavior in A5052 Aluminum Alloy with Diamond-Like Carbon/Anodic-Oxide Hybrid Coating, *Mater. Trans.*, 2015, **56**, p 1793–1799.
9. H. Maruno, and A. Nishimoto, Adhesion and Durability of Multi-interlayered Diamond-Like carbon Films Deposited on Aluminum Alloy, *Surf. Coat. Technol.*, 2018, **354**, p 134–144.
10. D.C. Lugo, P.C. Silva, M.A. Ramirez, E.J.D.M. Pillaca, C.L. Rodrigues, N.K. Fukumasu, E.J. Corat, M.H. Tabacniks, and V.J. Trava-Airoldi, Characterization and Tribologic Study in High Vacuum of Hydrogenated DLC Films Deposited using Pulsed DC PECVD System for Space Applications, *Surf. Coat. Technol.*, 2017, **332**, p 135–141.
11. I.S. Kannan, and A. Ghosh, Impact of Intra-Bond Orbital Hybridization and Morphology of Diamond Coatings on Machining Performance of Coated End Mill Cutters, *Int. J. Refract. Met. H.*, 2017, **68**, p 130–141.
12. O.V. Penkov, V.E. Pukha, S.L. Starikova, M. Khadem, V.V. Starikov, M.V. Maleev, and D.-E. Kim, Highly Wear-Resistant and Biocompatible Carbon Nanocomposite Coatings for Dental Implants, *Biomaterials*, 2016, **102**, p 130–136.
13. S.V. Hainsworth,, and N.J. Uhure, Diamond Like Carbon Coatings for Tribology: Production Techniques, Characterisation Methods and Applications, *Int. Mater. Rev.*, 2007, **52**, p 153–174.
14. X. Zha, F. Jiang, and X. Xu, Investigating the High Frequency Fatigue Failure Mechanisms of Mono and Multilayer PVD Coatings by the Cyclic Impact Tests, *Surf. Coat. Technol.*, 2018, **344**, p 689–701.
15. D.Q. Tan, X.Q. Yang, Q. He, J.L. Mo, W.H. Zhuang, and J.F. He, Impact-Sliding Wear Properties of PVD CrN and WC/C Coatings, *Surf. Eng.*, 2019 https://doi.org/10.1080/02670844.2019.1682818
16. R. Hauert, K. Thorwarth, and G. Thorwarth, An Overview on Diamond-Like Carbon Coatings in Medical Applications, *Surf. Coat. Technol.*, 2013, **233**, p 119–130.
17. S.D. Castellanos, A.J. Cavaleiro, A.M.P. de Jesus, R. Neto, and J. Lino Alves, Machinability of Titanium Aluminides: A Review, *P. I. Mech. Eng. L-J. Mat.*, 2019, **233**, p 426–451.
18. J. Li, X. Yu, Z.Q. Zhang, and Z.Y. Zhao, Exploring a Diamond Film to Improve Wear Resistance of the Hydraulic Drilling Impactor, *Surf. Coat. Technol.*, 2019, **360**, p 297–306.
19. Y. Chen, and X. Nie, Study of the Fatigue Wear Behaviors of a Tungsten Carbide Diamond-Like Carbon Coating on 316L Stainless Steel, *J. Vac. Sci. Technol. A.*, 2012, **30**, p 051506.
20. A.C. Hee, Y. Zhao, D. Choudhury, S. Ghosh, Q. Zhu, and H. Zhu, Tribological Behavior of Hydrogenated Diamond-Like Carbon on Polished Alumina Substrate with Chromium Interlayer for Biomedical Application, *Biotribology*, 2016, **7**, p 1–10.
21. D. Das, and A. Banerjee, Anti-Reflection Coatings for Silicon Solar Cells from Hydrogenated Diamond Like Carbon, *Appl. Surf. Sci.*, 2015, **345**, p 204–215.
22. H. Okubo, R. Tsuboi, and S.J.W. Sasaki, Frictional Properties of DLC Films in Low-Pressure Hydrogen Conditions, *Wear*, 2015 https://doi.org/10.1016/j.wear.2015.03.018
23. X. Wei, L. Chen, M. Zhang, Z. Lu, and G. Zhang, Effect of Dopants (F, Si) Material on the Structure and Properties of Hydrogenated DLC Film by Plane Cathode PECVD, *Diam. Relat. Mater.*, 2020, **110**, p 108102.
24. X.J. Cui, C.M. Ning, L.L. Shang, G.A. Zhang, and X.Q. Liu, Performance, Structure and Anticorrosion, Friction, and Wear Characteristics of Pure Diamond-Like Carbon (DLC), Cr-DLC, and Cr-HDLC Films on AZ91D Mg Alloy, *j. Mater. Eng. Perform.*, 2019 https://doi.org/10.1007/s11665-019-3854-8
25. J.L. Mo, M.H. Zhu, A. Leyland,, and A. Matthews, Impact Wear and Abrasion Resistance of CrN, AlCrN and AlTiN PVD Coatings, *Surf. Coat. Technol.*, 2013, **215**, p 170–177.
26. X. Sui, J. Liu, S. Zhang, J. Yang, and J. Hao, Microstructure, Mechanical and Tribological Characterization of CrN/DLC/Cr-DLC Multilayer Coating with Improved Adhesive Wear Resistance, *Appl. Surf. Sci.*, 2018, **439**, p 24–32.
27. J. Heinrichs, H. Mikado, A. Kawakami, U. Wiklund, S. Kawamura, and S. Jacobson, Wear Mechanisms of WC-Co Cemented Carbide Tools and PVD Coated Tools used for Shearing Cu-Alloy Wire in Zipper Production, *Wear*, 2019, **420**, p 96–107.
28. Z. Wang, Z.B. Cai, Y. Sun, J.F. Peng, and M.H. Zhu, Low Velocity Impact Wear Behavior of MoS_2/Pb Nanocomposite Coating under Controlled Kinetic Energy, *Surf. Coat. Technol.*, 2017, **326**, p 53–62.
29. O. Knotek, B. Bosserhoff, A. Schrey, T. Leyendecker, O. Lemmer, and S. Esser, A New Technique for Testing the Impact Load of Thin Films the Coating Impact Test, *Surf. Coat. Technol.*, 1992, **54**, p 102–107.
30. Y. Chen,, and X. Nie, Study on Fatigue and Wear Behaviors of a TiN Coating Using an Inclined Impact-Sliding Test, *Surf. Coat. Technol.*, 2011, **206**, p 1977–1982.
31. Y. Chen, X. Nie, A. Leyland, J. Housden, and A. Matthews, Substrate and Bonding Layer Effects on Performance of DLC and TiN Biomedical Coatings in Hank's Solution under Cyclic Impact-Sliding Loads, *Surf. Coat. Technol.*, 2013, **237**, p 219–229.
32. Z. Wang, Z. Cai, Y. Sun, S. Wu, and M. Zhu, Dynamic Response and Wear Behavior of Cr-DLC Coating under Impact Kinetic Energy Controlled Mode, China, *Surf. Eng.*, 2017, **30**, p 78–86.
33. T. Noguchi, K. Shimizu, N. Takahashi, and T. Nakamura, Strength Evaluation Of Cast Iron Grinding Balls by Repeated Drop Tests, *Wear*, 1999, **231**, p 301–309.
34. B.D. Beake, A. Bird, L. Isern, J.L. Endrino, and F. Jiang, Elevated Temperature Micro-Impact Testing of TiAlSiN Coatings Produced by Physical Vapour Deposition, *Thin Solid Films*, 2019, **688**, p 137358–137358.
35. J.P. Best, G. Guillonneau, S. Grop, A.A. Taylor, D. Frey, Q. Longchamp, T. Schär, M. Morstein, J.M. Breguet, and J. Michler, High temperature Impact Testing of a Thin Hard Coating using a Novel High-Frequency In Situ Micromechanical Device, *Surf. Coat. Technol.*, 2018, **333**, p 178–186.
36. Q.L. Li, S.M. Shi, X. Li, S.Y. Ding, C.L. Fan, and G.A. Zhang, Study on Low Velocity Cyclic Impact Wear of Amorphous Carbon Films with Different Mechanical Properties, *Surf. Coat. Technol.*, 2020, **402**, p 126339.
37. Z. Li, Y. Wang, X. Cheng, Z. Zeng, J. Li, X. Lu, L. Wang, and Q. Xue, Continuously Growing Ultrathick CrN Coating to Achieve High Load-Bearing Capacity and Good Tribological Property, *ACS. Appl. Mater. Inter.*, 2018, **10**, p 2965–2975.
38. N. Dwivedi, S. Kumar, and H.K. Malik, Nanoindentation Measurements on Modified Diamond-Like Carbon Thin Films, *Appl. Surf. Sci.*, 2011, **257**, p 9953–9959.
39. M.H. Staia, E.S. Puchi Cabrera, A. Iost, A. Zairi, S. Belayer, and A. Van Gorp, Tribological Response of AA 2024–T3 Aluminium Alloy Coated with a DLC Duplex Coating, *Tribol. Int.*, 2015, **85**, p 74–87.
40. W. Peng, W. Xia, X. Tao, W. Liu, and J. Zhang, Comparing Internal Stress in Diamond-Like Carbon Films with Different Structure, *Thin Solid Films*, 2007, **515**, p 6899–6903.
41. S. Neuville, and A. Matthews, A Perspective on the Optimisation of Hard Carbon and Related Coatings for Engineering Applications, *Thin Solid Films*, 2007, **515**, p 6619–6653.
42. H. Cao, F. Qi, X. Ouyang, N. Zhao, Y. Zhou, B. Li, W. Luo, B. Liao, and J. Luo, Effect of Ti Transition Layer Thickness on the Structure, Mechanical and Adhesion Properties of Ti-DLC Coatings on Aluminum Alloys, *Materials*, 2018, **11**, p 1742.
43. J.J. Wang, X. Li, G.Z. Wu, Z.B. Lu, G.G. Zhang, and Q.J. Xue, Origin of Low Friction for Amorphous Carbon Films with Different Hydrogen Content in Nitrogen Atmosphere, *Tribol. Int.*, 2019, **140**, p 105853.

44. D.C. Sutton, G. Limbert, B. Burdett, and R.J.W. Wood, Interpreting the Effects of Interfacial Chemistry on the Tribology of Diamond-Like Carbon Coatings Against Steel in Distilled Water, *Wear*, 2013, **302**, p 918–928.
45. S. Zhang, D. Sun, Y. Fu, and H. Du, Toughness Measurement of Thin Films: A Critical Review, *Surf. Coat. Technol.*, 2005, **198**, p 74–84.